Growth and Remodeling of Intracranial Saccular Aneurysms

Antonio DiCarlo[1], Vittorio Sansalone[2], Amabile Tatone[3],and Valerio Varano[*,1]
[1]LaMS – Modelling & Simulation Lab, Università Roma Tre, Italy,
[2]Laboratoire de Mécanique Physique, Université Paris Est, France,
[3]DISAT, Università degli Studi dell'Aquila, Italy.
[*]Corresponding author: via C. Segre 4, 00146 Roma, Italy, v.varano@uniroma3.it

Abstract: We present a mechanical model—a growing spherical shell—suitable for predicting the evolution of a Saccular Cerebral Artery Aneurysms (SCAA). It relies basically on the Kröner-Lee decomposition, used to describe the interplay between the current and the relaxed configuration of body elements. Rupture or stabilization of a SCAA are the end effect of a number of biological mechanisms, still poorly understood. We propose a model based on three competing remodeling mechanisms—one passive and two active. Despite drastic simplifying assumptions, preliminary numerical experiments attest to the potential of our model to account for nontrivial evolutions ensuing from accidental perturbations of a homeostatic state.

Keywords: Material remodeling, growth mechanics, spherical shells, soft tissue, saccular aneurysms

1 Introduction

We discuss the computational issues related to the implementation of a highly simplified mathematical caricature of a saccular cerebral artery aneurysm: a spherical thick shell susceptible of growth and remodelling. Aneurysms are lesions of the arterial wall having the form of a balloon-like pouch (saccular aneurysms) or of a barrel-like dilation (fusiform aneurysms). While an aneurysm forms and evolves, the arterial wall undergoes numerous morphological changes. The final fate of the lesion depends essentially on the capability of the arterial wall tissue to adapt to such changes. We focus on the two-way coupling between growth and stress, which we model within a theory in which bulk growth is governed by a novel balance law, i.e., the balance of remodelling couples. It relies basically on the Krner-Lee decomposition (1), used to describe the interplay between the current and the relaxed configuration of body elements. We propose a model based on three competing growth mechanisms, which we call decay, recovery and apposition. The first one is passive, describing a degradation of the tissue, while the other two arise as a response of the biochemical control system to changes in the hoop stress (which is the dominant stress component). We assume the material to be elastically incompressible and the problem to be spherically symmetric. By using spherical coordinates we obtain a one-dimensional evolution problem where the only significant spatial coordinate is the radial one. The thick shell is subjected to an intramural pressure–the blood pressure inside the aneurysm–, and a smaller extramural pressure–the intracranial pressure.

2 Geometry & kinematics

To satisfy a priori the spherical symmetry constraint, we conceive of a *reference shape* $\mathscr{D}$ of the vessel $\mathfrak{B}$ consisting in the (open) difference of two balls centered at $\boldsymbol{x}_{\circ} \in \mathscr{E}$, the three-dimensional Euclidean ambient space. Let ξ_-, ξ_+ be the radii of the two balls, with $0 < \xi_- < \xi_+ < \infty$. From now on, we shall identify each body-point $\mathfrak{b}$ in $\mathfrak{B}$ and on its boundary $\partial\mathfrak{B}$ with its place in $\boldsymbol{x} \in \overline{\mathscr{D}}$ (the closure of $\mathscr{D}$). In turn, each place $\boldsymbol{x} \in \overline{\mathscr{D}}$ will be identified with the triple of its spherical coordinates $(\xi, \vartheta, \varphi)$, where ξ is the distance from the center $\boldsymbol{x}_{\circ}$ (or *radius*) and ϑ, φ are the coordinates of its projection on the unit sphere. All spherically symmetric vector fields $\boldsymbol{v} : \overline{\mathscr{D}} \to \mathsf{V}\mathscr{E}$ (with $\mathsf{V}\mathscr{E}$ the translation space of $\mathscr{E}$) and tensor fields $\mathbf{L} : \overline{\mathscr{D}} \to \mathsf{V}\mathscr{E} \otimes \mathsf{V}\mathscr{E}$ admit the following representation:

$$\boldsymbol{v}(\boldsymbol{x}) = v(\xi)\, \boldsymbol{e}_r(\vartheta, \varphi)\,, \tag{1}$$

$$\mathbf{L}(\boldsymbol{x}) = \mathrm{L}_r(\xi)\, \mathbf{P}_r(\vartheta, \varphi) + \mathrm{L}_h(\xi)\, \mathbf{P}_h(\vartheta, \varphi)\,, \tag{2}$$

respectively, $\boldsymbol{e}_r$ being the unit outward radial vector field, and $\mathbf{P}_r := \boldsymbol{e}_r \otimes \boldsymbol{e}_r$, $\mathbf{P}_h := \mathbf{I} - \mathbf{P}_r$ the

orthogonal projectors of $\mathsf{V}\mathscr{E}\otimes\mathsf{V}\mathscr{E}$ onto the *radial* direction and the *hoop* directions, respectively (with $\mathbf{I}$ the identity on $\mathsf{V}\mathscr{E}$). All *gross placement* of $\mathfrak{B}$ will be described through the corresponding *transplacement* $\mathsf{p}:\overline{\mathscr{D}}\times[\,0,\tau_+[\,\subset\mathscr{T}\to\mathscr{E}$:

$$\mathsf{p}(\boldsymbol{x},\tau)\;=\;\boldsymbol{x}_\circ+\rho\,(\xi,\tau)\,\boldsymbol{e}_r(\vartheta,\varphi)\,,\qquad(3)$$

where $\mathscr{T}$ is the (real) *time line*, and $0<\tau_+\leq\infty$ is the *duration* of the process. The smooth, strictly positive real-valued *radius-to-radius map* $\rho:[\,\xi_-,\xi_+]\times[\,0,\tau_+[\,\to\mathbb{R}^+$, is assumed to be such that $\rho\,(\,\cdot\,,\tau)$ is monotonically increasing. Consequently, the *transplacement gradient* is the spherically symmetric, positive-valued tensor field

$$\begin{aligned}\nabla\mathsf{p}(\boldsymbol{x},\tau)=\rho'(\xi,\tau)\,\mathbf{P}_r(\vartheta,\varphi)\\+\frac{\rho}{\xi}(\xi,\tau)\,\mathbf{P}_h(\vartheta,\varphi)\,,\end{aligned}\qquad(4)$$

where a prime denotes radial differentiation. To make precise the idea of an evolving relaxed state, we introduce the smooth, positive-valued tensor field

$$\begin{aligned}\mathbf{G}:(\boldsymbol{x},\tau)\mapsto\gamma_r(\xi,\tau)\,\mathbf{P}_r(\vartheta,\varphi)\\+\gamma_h(\xi,\tau)\,\mathbf{P}_h(\vartheta,\varphi)\,,\end{aligned}\qquad(5)$$

which we call *relaxed transplant*. The (positive-valued) radial and hoop *transformation stretches* γ_r and γ_h gauge the discrepancy between the relaxed state and the reference configuration. We introduce the *relaxed Jacobian*

$$\begin{aligned}J(\boldsymbol{x},\tau)&:=\det\mathbf{G}(\boldsymbol{x},\tau)\\&=\gamma_r(\xi,\tau)\,\gamma_h(\xi,\tau)^2\end{aligned}\qquad(6)$$

From now on, time τ and/or reference position $\boldsymbol{x}$ (or its coordinates (ξ,ϑ,φ)) will be dropped from notation whenever unambiguously inferable from the context. The Kröner-Lee decomposition defines the *warp*

$$\mathbf{F}:=\nabla\mathsf{p}\mathbf{G}^{-1}=\lambda_r\,\mathbf{P}_r+\lambda_h\,\mathbf{P}_h\,,\qquad(7)$$

where the radial and hoop *effective stretches* are given by the (positive) ratios:

$$\lambda_r:=\frac{\rho'}{\gamma_r}\,,\qquad\lambda_h:=\frac{\rho}{\xi\,\gamma_h}\,,\qquad(8)$$

respectively. Of course, $\mathbf{F}$ is a gradient if and only if $\mathbf{G}$ is. The actual configuration at time τ is stress-free if and only if $\mathbf{F}(\boldsymbol{x},\tau)=\mathbf{I}$ for all $\boldsymbol{x}\in\overline{\mathscr{D}}$. The *velocity* realized along the refined motion $(\mathsf{p},\mathbf{G})$ is, by definition, the pair consisting of the *gross velocity* $\dot{\mathsf{p}}$ and the *growth velocity* $\dot{\mathbf{G}}\,\mathbf{G}^{-1}$ (a superposed dot denoting time differentiation):

$$\begin{aligned}\dot{\mathsf{p}}&=\dot\rho\;\boldsymbol{e}_r\,,\\\dot{\mathbf{G}}\,\mathbf{G}^{-1}&=\frac{\dot\gamma_r}{\gamma_r}\,\mathbf{P}_r+\frac{\dot\gamma_h}{\gamma_h}\,\mathbf{P}_h\,,\end{aligned}\qquad(9)$$

2.1 Multiple remodeling mechanisms

As a first attempt to mimic the homestatic mechanisms presiding over the evolution of saccular aneurysms, we split $\mathbf{G}$ into three factors:

$$\mathbf{G}=\mathbf{G}_\mathfrak{a}\,\mathbf{G}_\mathfrak{r}\,\mathbf{G}_\mathfrak{d}\,,\qquad(10)$$

corresponding respectively to *decay* ($\mathfrak{d}$), *recovery* ($\mathfrak{r}$), and *apposition* ($\mathfrak{a}$). The *decay transplant* $\mathbf{G}_\mathfrak{d}$ is meant to provide a creep-like caricature of the kinematical effects of tissue damage, due to any biophysical reasons (*e.g.*, decay of collagen fibers). It is assumed to be isochoric:

$$\begin{aligned}J_\mathfrak{d}:=\det\mathbf{G}_\mathfrak{d}=1\quad\Leftrightarrow\\\mathbf{G}_\mathfrak{d}=\gamma_\mathfrak{d}^{-2}\,\mathbf{P}_r+\gamma_\mathfrak{d}\,\mathbf{P}_h\,.\end{aligned}\qquad(11)$$

The *recovery transplant* $\mathbf{G}_\mathfrak{r}$ is representative of a hypothetical mechanobiological feedback aiming at countering the effects of tissue damage. Also this transplant is assumed to be isochoric:

$$\begin{aligned}J_\mathfrak{r}:=\det\mathbf{G}_\mathfrak{r}=1\quad\Leftrightarrow\\\mathbf{G}_\mathfrak{r}=\gamma_\mathfrak{r}^{-2}\,\mathbf{P}_r+\gamma_\mathfrak{r}\,\mathbf{P}_h\,.\end{aligned}\qquad(12)$$

The *apposition transplant* $\mathbf{G}_\mathfrak{a}$ accounts for new tissue deposition, triggered, *e.g.*, by an occasional shift from an established homeostatic state. This transplant is supposed to act trivially in the hoop directions

$$\begin{aligned}\mathbf{G}_\mathfrak{a}=\gamma_\mathfrak{a}\,\mathbf{P}_r+\mathbf{P}_h\quad\Rightarrow\\J_\mathfrak{a}:=\det\mathbf{G}_\mathfrak{a}=\gamma_\mathfrak{a}\,.\end{aligned}\qquad(13)$$

Substituting Eqs. (11), (12), and (13) into Eq. (10), we get the representation

$$\mathbf{G}=\gamma_\mathfrak{a}(\gamma_\mathfrak{d}\gamma_\mathfrak{r})^{-2}\,\mathbf{P}_r+\gamma_\mathfrak{d}\gamma_\mathfrak{r}\,\mathbf{P}_h\,,\qquad(14)$$

showing how the relaxed transplant $\mathbf{G}$ is parameterized by three independent scalar fields: the *hoop decay stretch* $\gamma_\mathfrak{d}$, the *hoop recovery stretch* $\gamma_\mathfrak{r}$, and the *radial apposition stretch* $\gamma_\mathfrak{a}$. Time differentiation of Eq. (14) leads to

the following representation of the growth velocity realized along the refined motion:

$$\dot{\mathbf{G}}\,\mathbf{G}^{-1} = \left(\frac{\dot\gamma_{\mathfrak{a}}}{\gamma_{\mathfrak{a}}} - 2\left(\frac{\dot\gamma_{\mathfrak{d}}}{\gamma_{\mathfrak{d}}} + \frac{\dot\gamma_{\mathfrak{r}}}{\gamma_{\mathfrak{r}}}\right)\right)\mathbf{P}_r + \left(\frac{\dot\gamma_{\mathfrak{d}}}{\gamma_{\mathfrak{d}}} + \frac{\dot\gamma_{\mathfrak{r}}}{\gamma_{\mathfrak{r}}}\right)\mathbf{P}_h\,. \tag{15}$$

3 Working & balance

Let $\mathfrak{T}$ be the linear space of instantaneous *test velocities* comprising all smooth fields $\boldsymbol{x} \mapsto (\boldsymbol{v}, \mathbf{V}_{\mathfrak{d}}, \mathbf{V}_{\mathfrak{r}}, \mathbf{V}_{\mathfrak{a}})$, with $\boldsymbol{v}$ the gross velocity, $\mathbf{V}_{\mathfrak{d}}$ the *decay velocity*, $\mathbf{V}_{\mathfrak{r}}$ the *recovery velocity*, and $\mathbf{V}_{\mathfrak{a}}$ the *apposition velocity*. To get rid of reactive accretive couples, we evaluate the power expended on the *restricted test space* comprised of growth velocities parameterized by the *hoop decay stretching* $\nu_{\mathfrak{d}}$:

$$\mathbf{V}_{\mathfrak{d}} = \nu_{\mathfrak{d}}(\mathbf{P}_h - 2\,\mathbf{P}_r)\,, \tag{16}$$

the *hoop recovery stretching* $\nu_{\mathfrak{r}}$:

$$\mathbf{V}_{\mathfrak{r}} = \nu_{\mathfrak{r}}(\mathbf{P}_h - 2\,\mathbf{P}_r)\,, \tag{17}$$

and the *radial apposition stretching* $\nu_{\mathfrak{a}}$:

$$\mathbf{V}_{\mathfrak{a}} = \nu_{\mathfrak{a}}\,\mathbf{P}_r\,. \tag{18}$$

Because of the compound structure of test velocities, force splits additively into a *brute force*, dual to $\boldsymbol{v}$, and an *accretive force*, dual to $\mathbf{V}$. The working expended on $(\boldsymbol{v}, \mathbf{V})$ is assumed to be represented by

$$\int_{\mathscr{D}} (-\mathbf{S}\cdot\nabla\boldsymbol{v}) + \int_{\partial\mathscr{D}} \boldsymbol{t}_{\partial\mathscr{D}}\cdot\boldsymbol{v} + \int_{\mathscr{D}} J(\mathbb{A}_{\mathfrak{d}}\cdot\mathbf{V}_{\mathfrak{d}} + \mathbb{A}_{\mathfrak{r}}\cdot\mathbf{V}_{\mathfrak{r}} + \mathbb{A}_{\mathfrak{a}}\cdot\mathbf{V}_{\mathfrak{a}})\,. \tag{19}$$

The *accretive couples* per unit reference volume $\mathbb{A}_{\mathfrak{d}}$, $\mathbb{A}_{\mathfrak{r}}$, $\mathbb{A}_{\mathfrak{a}}$ and the *reference Piola stress* $\mathbf{S}$ (also a specific couple) take values in $\mathsf{V}\mathscr{E}\otimes\mathsf{V}\mathscr{E}$; the (brute) *boundary-force* per unit reference area $\boldsymbol{t}_{\partial\mathscr{D}}$ takes values in $\mathsf{V}\mathscr{E}$. The accretive couple working per unit reference volume can be given the expression:

$$J(\mathbb{A}_{\mathfrak{d}}\cdot\mathbf{V}_{\mathfrak{d}} + \mathbb{A}_{\mathfrak{r}}\cdot\mathbf{V}_{\mathfrak{r}} + \mathbb{A}_{\mathfrak{a}}\cdot\mathbf{V}_{\mathfrak{a}}) = J(\mathcal{A}_{\mathfrak{d}}\nu_{\mathfrak{d}} + \mathcal{A}_{\mathfrak{r}}\nu_{\mathfrak{r}} + \mathcal{A}_{\mathfrak{a}}\nu_{\mathfrak{a}})\,, \tag{20}$$

where the scalar fields $\mathcal{A}_{\mathfrak{d}}, \mathcal{A}_{\mathfrak{r}}, \mathcal{A}_{\mathfrak{a}}$ are the *effective* accretive couples per unit *relaxed* volume:

$$\mathcal{A}_{\mathfrak{d}} = \mathbb{A}_{\mathfrak{d}}\cdot(\mathbf{P}_h - 2\,\mathbf{P}_r) = 2\,(\mathrm{A}_{\mathfrak{d}h} - \mathrm{A}_{\mathfrak{d}r})\,, \tag{21}$$

$$\mathcal{A}_{\mathfrak{r}} = \mathbb{A}_{\mathfrak{r}}\cdot(\mathbf{P}_h - 2\,\mathbf{P}_r) = 2\,(\mathrm{A}_{\mathfrak{r}h} - \mathrm{A}_{\mathfrak{r}r})\,, \tag{22}$$

$$\mathcal{A}_{\mathfrak{a}} = \mathbb{A}_{\mathfrak{a}}\cdot\mathbf{P}_r = \mathrm{A}_{\mathfrak{a}r}\,, \tag{23}$$

dual respectively to the decay, recovery, and apposition stretching. Balance laws are systematically provided by the *balance principle* stating that, at each time, the working expended on any test velocity should be zero. Via standard localization arguments, this yields the local statements of balance of brute forces and accretive couples:

$$2\,\big(\mathrm{S}_r(\xi) - \mathrm{S}_h(\xi)\big) + \xi\,\mathrm{S}_r'(\xi) = 0\,, \tag{24}$$

$$\begin{aligned}\mathcal{A}_{\mathfrak{d}} &= \mathcal{A}_{\mathfrak{d}}^{\mathrm{i}} + \mathcal{A}_{\mathfrak{d}}^{\mathrm{o}} = 0\,,\\ \mathcal{A}_{\mathfrak{r}} &= \mathcal{A}_{\mathfrak{r}}^{\mathrm{i}} + \mathcal{A}_{\mathfrak{r}}^{\mathrm{o}} = 0\,,\\ \mathcal{A}_{\mathfrak{a}} &= \mathcal{A}_{\mathfrak{a}}^{\mathrm{i}} + \mathcal{A}_{\mathfrak{a}}^{\mathrm{o}} = 0\,,\end{aligned} \tag{25}$$

for all $\xi_- < \xi < \xi_+$, and

$$\mathrm{S}_r(\xi_\mp) = -\,\pi_\mp\,, \tag{26}$$

where S_r is the *radial* and S_h the *hoop* component of the reference stress $\mathbf{S}$ (the same attributes apply to the homonymous components of accretive couples), and (plus or minus) the *outer reference pressure* π is the only strict component of the boundary force per unit reference area:

$$\boldsymbol{t}_{\partial\mathscr{D}}(\boldsymbol{x}_{\mathrm{o}} + \xi_\mp\boldsymbol{e}_r(\vartheta,\varphi)) = \pm\,\pi_\mp\,\boldsymbol{e}_r(\vartheta,\varphi)\,. \tag{27}$$

The total couples $\mathcal{A}_{\mathfrak{d}}$, $\mathcal{A}_{\mathfrak{r}}$, $\mathcal{A}_{\mathfrak{a}}$ have been split into the sum of an inner and an outer contribution. The distinction between them belongs in the constitutive theory

4 Constitutive issues

4.1 Constitutive theory: energetics

To parameterize the state of the body, we postulate the existence of a real-valued free-energy measure, such that the energy available to any part $\mathscr{P}$ of $\mathscr{D}$ is given by

$$\Psi(\mathscr{P}) = \int_{\mathscr{P}} J\,\psi\,, \tag{28}$$

where the density ψ represents the free energy per unit *relaxed* volume, so that $J\,\psi$ is the free energy per unit *reference* volume (recall Eq. (6)). We assume *the free-energy density $\psi(\boldsymbol{x},\tau)$ to depend solely on the actual value of the warp $\mathbf{F}(\boldsymbol{x},\tau)$ and on $\boldsymbol{x}$ itself*:

$$\psi(\boldsymbol{x},\tau) = \phi\,(\mathbf{F}(\boldsymbol{x},\tau), \boldsymbol{x})\,. \tag{29}$$

4.2 Constitutive theory: inner forces

The *dissipation principle* plays a primary role in the constitutive theory of inner forces:

$$\begin{aligned}&\mathbf{S}\cdot\nabla\dot{\mathsf{p}} - J\left(\mathcal{A}^{\mathfrak{i}}_{\mathfrak{d}}\,\frac{\dot\gamma_{\mathfrak{d}}}{\gamma_{\mathfrak{d}}} + \mathcal{A}^{\mathfrak{i}}_{\mathfrak{r}}\,\frac{\dot\gamma_{\mathfrak{r}}}{\gamma_{\mathfrak{r}}} + \mathcal{A}^{\mathfrak{i}}_{\mathfrak{a}}\,\frac{\dot\gamma_{\mathfrak{a}}}{\gamma_{\mathfrak{a}}}\right)\\ &- (J\,\psi)^{\cdot} \geq 0\,.\end{aligned} \tag{30}$$

Inequality (30) is satisfied along all refined motions if and only if the constitutive prescriptions for the Piola stress and the inner accretive couples have the following structure:

$$\mathbb{S} = (\mathsf{D}_1\phi)|_{\mathbf{F}} + \overset{+}{\mathbb{S}}\,, \tag{31}$$

$$\begin{aligned}\mathcal{A}^{\mathfrak{i}}_{\mathfrak{d}} &= 2\,(\mathrm{T}_h - \mathrm{T}_r) + \overset{+}{\mathcal{A}}_{\mathfrak{d}}\,,\\ \mathcal{A}^{\mathfrak{i}}_{\mathfrak{r}} &= 2\,(\mathrm{T}_h - \mathrm{T}_r) + \overset{+}{\mathcal{A}}_{\mathfrak{r}}\,,\\ \mathcal{A}^{\mathfrak{i}}_{\mathfrak{a}} &= \mathrm{T}_r - \phi + \overset{+}{\mathcal{A}}_{\mathfrak{a}}\,,\end{aligned} \tag{32}$$

where $\mathbb{S}$ denotes the *relaxed* Piola stress per unit *relaxed* volume:

$$\mathbb{S} := J^{-1}\mathbf{S}\,\mathbf{G}^{\top}, \tag{33}$$

$\mathsf{D}_1\phi$ is the derivative of ϕ with respect to its first argument, T_h and T_r are the components of the *Cauchy stress*

$$\begin{aligned}\mathbf{T} &:= (\det\mathbf{F})^{-1}\mathbb{S}\,\mathbf{F}^{\top}\\ &= (\det\nabla\mathsf{p})^{-1}\mathbf{S}\,(\nabla\mathsf{p})^{\top},\end{aligned} \tag{34}$$

and the constitutive prescriptions for the *dissipative* components $\overset{+}{\mathbb{S}}$ and $\overset{+}{\mathbb{A}}$ identically satisfy the *reduced dissipation inequality*:

$$\overset{+}{\mathbb{S}}\cdot\dot{\mathbf{F}} - \left(\overset{+}{\mathcal{A}}_{\mathfrak{d}}\,\frac{\dot\gamma_{\mathfrak{d}}}{\gamma_{\mathfrak{d}}} + \overset{+}{\mathcal{A}}_{\mathfrak{r}}\,\frac{\dot\gamma_{\mathfrak{r}}}{\gamma_{\mathfrak{r}}} + \overset{+}{\mathcal{A}}_{\mathfrak{a}}\,\frac{\dot\gamma_{\mathfrak{a}}}{\gamma_{\mathfrak{a}}}\right) \geq 0\,. \tag{35}$$

We assume the inner brute force to be *hyperelastic*, *i.e.*,

$$\overset{+}{\mathbb{S}} = 0\,. \tag{36}$$

Following (2), we assume the aneurysm wall to be *elastically incompressible*, enforcing the constraint

$$\det\mathbf{F} = \lambda_r\lambda_h^2 = 1 \quad\Leftrightarrow\quad \lambda_r = \lambda_h^{-2}, \tag{37}$$

and restricting ϕ to the submanifold $\mathscr{U}$ of (spherical symmetric) *unimodular* warps parameterized by the hoop stretch λ as follows:

$$\mathscr{U} \ni \mathbf{F} = \lambda^{-2}\,\mathbf{P}_r + \lambda\,\mathbf{P}_h\,, \tag{38}$$

$$\begin{aligned}&\phi|_{\mathscr{U}}(\mathbf{F}(\boldsymbol{x}),\boldsymbol{x})\\ &= k\left\{\exp\left[\alpha\big(\lambda(\xi)^2-1\big)^2\right]-1\right\}.\end{aligned} \tag{39}$$

The incompressibility constraint (37) is maintained by a reactive inner force. The set of reactions is parameterized by a scalar field, the *reactive pressure* p, so that the Cauchy stress is now:

$$\mathbf{T} = (\mathsf{D}_1\phi|_{\mathscr{U}})|_{\mathbf{F}}\,\mathbf{F}^{\top} - p\,\mathbf{I}\,, \tag{40}$$

4.3 Constitutive characterization of effective accretive couples

We assume decay ($\mathfrak{d}$), recovery ($\mathfrak{r}$), and apposition ($\mathfrak{a}$) mechanisms to be *uncoupled* from each other. In our preliminary numerical experiments (see Sect. 6) we simply assume:

$$\overset{+}{\mathcal{A}}_{\mathfrak{d}} = -\,d_{\mathfrak{d}}\,\frac{\dot\gamma_{\mathfrak{d}}}{\gamma_{\mathfrak{d}}}\,,\ \overset{+}{\mathcal{A}}_{\mathfrak{r}} = -\,d_{\mathfrak{r}}\,\frac{\dot\gamma_{\mathfrak{r}}}{\gamma_{\mathfrak{r}}}\,,\ \overset{+}{\mathcal{A}}_{\mathfrak{a}} = -\,d_{\mathfrak{a}}\,\frac{\dot\gamma_{\mathfrak{a}}}{\gamma_{\mathfrak{d}}}$$

$$\text{with}\quad d_{\mathfrak{d}} > 0\,,\ \ d_{\mathfrak{r}} > 0\,,\ \ d_{\mathfrak{a}} > 0\,.$$

The remaining constitutive ingredient is the prescription for the outer accretive couples $\mathcal{A}^{\mathfrak{o}}_{\mathfrak{d}}$, $\mathcal{A}^{\mathfrak{o}}_{\mathfrak{r}}$, $\mathcal{A}^{\mathfrak{o}}_{\mathfrak{a}}$ appearing in Eq. (25). We shall assume:

$$\begin{aligned}\mathcal{A}^{\mathfrak{o}}_{\mathfrak{d}}(\xi,\tau) &= 0\,,\\ \mathcal{A}^{\mathfrak{o}}_{\mathfrak{r}}(\xi,\tau) &= \widehat{\mathcal{A}}_{\mathfrak{r}}\big(\mathbf{T}(\xi,\tau),\mathbf{T}^{\diamond}(\xi,\tau),\tau\big)\,,\\ \mathcal{A}^{\mathfrak{o}}_{\mathfrak{a}}(\xi,\tau) &= \widehat{\mathcal{A}}_{\mathfrak{a}}\big(\mathbf{T}(\xi,\tau),\mathbf{T}^{\diamond}(\xi,\tau),\tau\big)\,.\end{aligned} \tag{41}$$

The first of Eqs. (41) declares that the decay mechanism is supposed to be *passive*. The other two hypothesize that the biomechanical feedback mechanisms controlling recovery and apposition are pointwise sensitive to the actual value of the Cauchy stress $\mathbf{T}$, in comparison with a supposedly known *homeostatic* stress $\mathbf{T}^{\diamond}$. In the following we explore numerically the most accessible consequences of some simplistic, but reasonable assumptions, such as:

$$\begin{aligned}\widehat{\mathcal{A}}_{\mathfrak{r}}\big(\mathbf{T},\mathbf{T}^{\diamond}\big) &= -\mathrm{E}_{\mathfrak{d}\&\mathfrak{r}}(\mathbf{T}) - f_{\mathfrak{r}}\,(\mathrm{T}_h - \mathrm{T}_h^{\diamond})\\ &\quad + c_{\mathfrak{r}}\frac{\rho-\bar\rho}{\rho'}\,(\mathrm{T}_h - \mathrm{T}_h^{\diamond})'\,,\end{aligned} \tag{42}$$

$$\widehat{\mathcal{A}}_{\mathfrak{a}}\big(\mathbf{T},\mathbf{T}^{\diamond}\big) = -\mathrm{E}_{\mathfrak{a}}(\mathbf{T}) + f_{\mathfrak{a}}\,(\mathrm{T}_h - \mathrm{T}_h^{\diamond})\,, \tag{43}$$

whose rationale is the idea that the homeostatic control senses pointwise the hoop component of the Cauchy stress T_h and of its radial derivative T_h', aiming to bring them back to their homeostatic values $\mathrm{T}_h^{\diamond}$ and $(\mathrm{T}_h^{\diamond})'$, respectively. The feedback coefficients $f_{\mathfrak{r}}$, $f_{\mathfrak{a}}$ and $c_{\mathfrak{r}}$ are assumed to be constant across the

thickness. Upon substitution of Eqs. (41) and (32) into Eq. (25), with $\overset{+}{\mathcal{A}}_{\mathfrak{d}}$, $\overset{+}{\mathcal{A}}_{\mathfrak{r}}$, $\overset{+}{\mathcal{A}}_{\mathfrak{a}}$ given by Eq. (4.3) and, finally, recalling Eq. (15), we readily obtain the set of equations determining the radial and hoop components of the growth velocity $\dot{\mathbf{G}}\,\mathbf{G}^{-1}$:

$$\begin{aligned} \frac{\dot\gamma_h}{\gamma_h} &= \frac{\mu_{\mathfrak{r}}}{d_{\mathfrak{d}}}\Big(\mathrm{E}_{\mathfrak{d}\&\mathfrak{r}}(\mathbf{T}) + \widehat{\mathcal{A}}_{\mathfrak{r}}\big(\mathbf{T},\mathbf{T}^{\diamond}\big)\Big), \\ \frac{\dot\gamma_r}{\gamma_r} + 2\,\frac{\dot\gamma_h}{\gamma_h} &= \frac{\mu_{\mathfrak{a}}}{d_{\mathfrak{d}}}\Big(\mathrm{E}_{\mathfrak{a}}(\mathbf{T}) + \widehat{\mathcal{A}}_{\mathfrak{a}}\big(\mathbf{T},\mathbf{T}^{\diamond}\big)\Big), \end{aligned} \tag{44}$$

where the positive *mobility ratios* $\mu_{\mathfrak{r}}$ and $\mu_{\mathfrak{a}}$ are defined as $\mu_{\mathfrak{r}} := d_{\mathfrak{d}}/d_{\mathfrak{r}}$, $\mu_{\mathfrak{a}} := d_{\mathfrak{d}}/d_{\mathfrak{a}}$, and the *Eshelby maps* $\mathrm{E}_{\mathfrak{d}\&\mathfrak{r}}$, $\mathrm{E}_{\mathfrak{a}}$ are defined by

$$\begin{aligned} \mathrm{E}_{\mathfrak{d}\&\mathfrak{r}}(\mathbf{T}) &:= 2\left(1+\mu_{\mathfrak{r}}^{-1}\right)(\mathrm{T}_h - \mathrm{T}_r), \\ \mathrm{E}_{\mathfrak{a}}(\mathbf{T}) &:= \mathrm{T}_r - \phi. \end{aligned} \tag{45}$$

5 Use of COMSOL Multiphysics

Our formulation is originally based on an integral balance principle. As a result, it finds a seamless and natural implementation in COMSOL by using the 1D PDE weak-form application mode as is, and then exploiting the capability of the time-dependent COMSOL solver. We use a mixed approach, interpolating independently the following scalar fields: the actual radius, the (hoop and radial) transformation stretches, the (hoop and radial) components of the Cauchy and Eshelby stresses, and the reactive pressure maintaining the incompressibility constraint. The solution algorithm is arranged in two successive steps, each encoded in a separate script file: the first computes the initial–supposedly homeostatic–state of the system, by solving a nonlinear semi-inverse equilibrium problem; the second integrates in time the evolution of the system–either benign or fatal–triggered by a perturbation of the initial homeostatic state, such as an intramural pressure peak or jump. Other script files manage the post-processing phase, making it easy to compare different simulations by arranging and displaying a number of graphs, such as those shown in the next section. This problem, though one-dimensional, is computationally far from trivial, being highly nonlinear.

6 Numerical simulations

We consider in our analysis a small size spherical aneurysm having attained a homeostatic state. Homeostasis is then perturbed and the ensuing evolution of the aneurysm is studied. The mean radius and the thickness in the paragon shape are assumed to be $(\xi_- + \xi_+)/2 = 2.0$ mm and $(\xi_- - \xi_+) = 20\,\mu$m, respectively (3). The moduli k and α in Eq.(39) are tuned by following (3). The intramural pressure and extramural pressure are assumed to be $\pi_- = 90\,$mmHg and $\pi_+ = 15\,$mmHg, respectively.

6.1 Initial Homeostatic state

The first step in each of the following simulations, accomplished by the script `dofem0`, consists in computing the initial ($\tau = 0$) homeostatic state. We suppose that a homeostatic state is characterized by a uniform hoop stress $T_h^{\diamond}$. For a fixed shape and given values for $\pi_{\pm}$, we search for the relaxed transplant making the corresponding stress (40), through the energy expression (39), satisfy the balance equations (24) and (26). It is worth noting that solving the balance equations above for a uniform hoop stress gives the *generalized Laplace formula*:

$$T_h^{\diamond} = \frac{\rho_+^2\,\pi_+ - \rho_-^2\,\pi_-}{\rho_-^2 - \rho_+^2} \tag{46}$$

By choosing the actual shape as the reference shape it turns out that $\nabla \mathsf{p} = \mathbf{I} \Rightarrow \mathbf{G} = \mathbf{F}^{-1}$. Then we can solve the balance equation (24) for the sole unknown γ_h, by using the COMSOL nonlinear stationary solver `femnlin`. Starting from the computed values for γ_h we finally reconstruct the whole initial homeostatic state.

6.2 Perturbation & Controls

In a second step homeostasis is perturbed by an intramural pressure jump, described by the smoothed step in Fig. 1, and a control mechanism try to bring the hoop stress back to the homeostatic value.

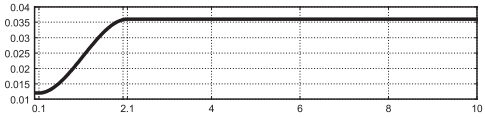

Figure 1: Intramural pressure jump.

This step is accomplished by the script `dofem1`, where the brute balance equation (24) and the evolution equations (44) are integrated by using the COMSOL time solver `femtime`. We show how different values for the feedback coefficients make the control succeed or not.

6.2.1 Recovery control-I

The first set of simulations was performed by choosing $f_{\mathfrak{a}} = 0$, $f_{\mathfrak{r}} > 0$ and $c_{\mathfrak{r}} = 0$: only the recovery control is activated and it does not sense the value of T'_h. The graphs in Fig. 2, 3 and 4 show why in this case the control does not work: it leads to diverging values of the hoop stress across the wall. Notice how the time cross-sections in Fig.4 show a progressive localization of the stress near the interior boundary (left).

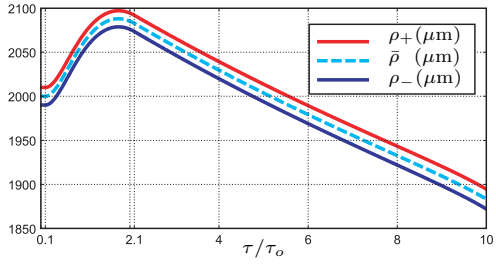

Figure 2: Actual radius vs time.

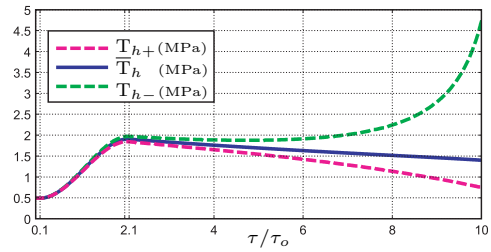

Figure 3: Hoop stress vs time.

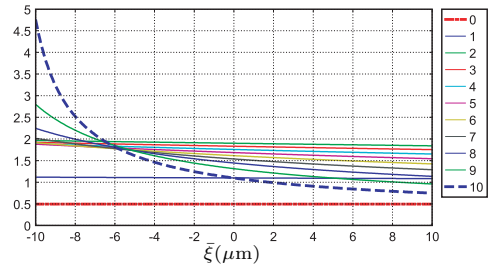

Figure 4: Hoop stress field.

6.2.2 Recovery control-II

The second set of simulations was performed by choosing $f_{\mathfrak{a}} = 0$, $f_{\mathfrak{r}} > 0$ and $c_{\mathfrak{r}} > 0$: only the recovery control is activated but now it senses the value of T'_h. As shown in Fig. 5, 6, 7, in this case the control works fine.

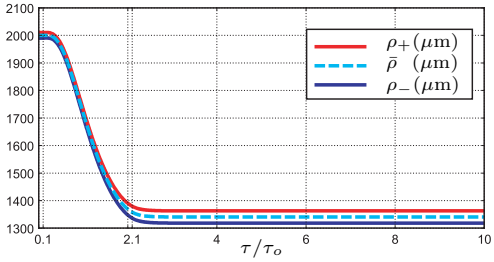

Figure 5: Actual radius vs time.

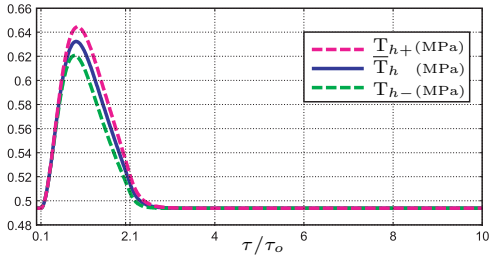

Figure 6: Hoop stress vs time.

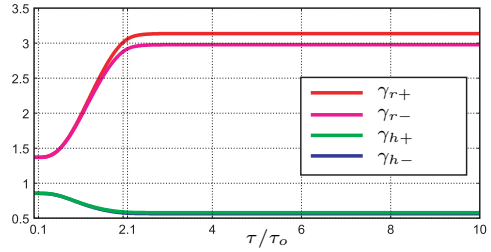

Figure 7: Transformation stretches vs time.

6.2.3 Apposition control

A third set of simulations was performed by choosing $f_{\mathfrak{a}} > 0$, $f_{\mathfrak{r}} = 0$ and $c_{\mathfrak{r}} = 0$: only the apposition control is activated and this, by definition (43), does not sense the value of T'_h. As the graphs in Fig. 8, 9 and 10 show, even in this case the control does not work: it leads again to diverging values of the hoop stress across the wall. The time cross-sections in Fig. 10 show a progressive localization of the stress near the exterior boundary (right). In fact, it is easy to prove by means of Eqs.(8, 39, 46) that it is impossible, after a change of boundary conditions, to restore the value of

T_h while leaving γ_h unchanged. Hence a control acting only in the radial direction cannot work.

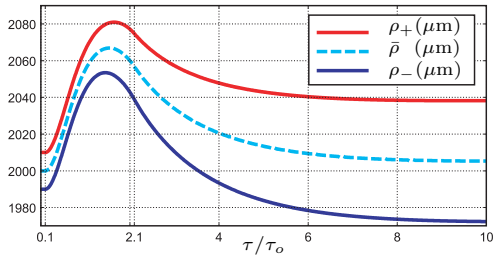

Figure 8: Actual radius vs time.

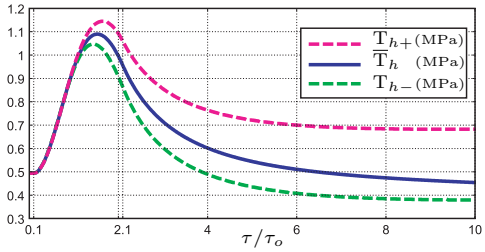

Figure 9: Hoop stress vs time.

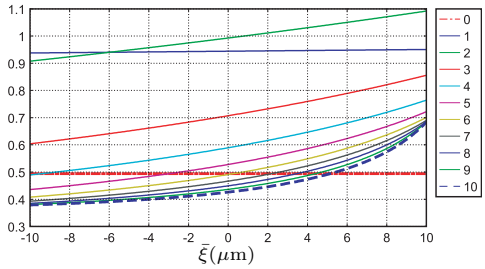

Figure 10: Hoop stress field.

6.2.4 Mixed control

The last set of simulations was performed by choosing $f_{\mathfrak{a}} > 0$, $f_{\mathfrak{r}} = 0$ and $c_{\mathfrak{r}} > 0$: the apposition control is activated and it is supported, in controlling the value of T'_h, by the recovery control. In this case the apposition affects the mean value of T_h, while the hoop recovery affects T'_h. The main difference between the two working control types (Recovery control-II and Mixed control) is that the first one leads to a decrease of the mean radius of the aneurysm, while the second one leads just to an increase of the thickness, that seems more realistic.

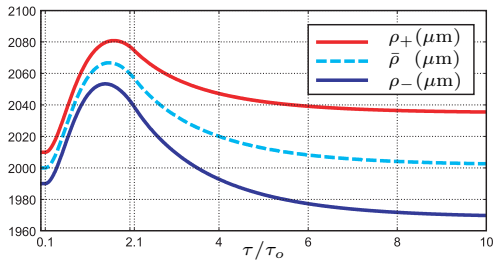

Figure 11: Actual radius vs time.

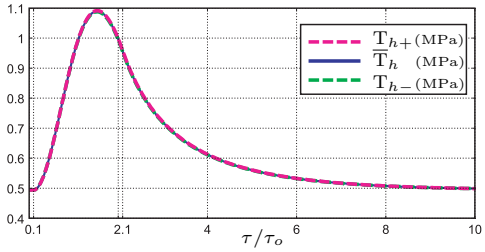

Figure 12: Hoop stress vs time.

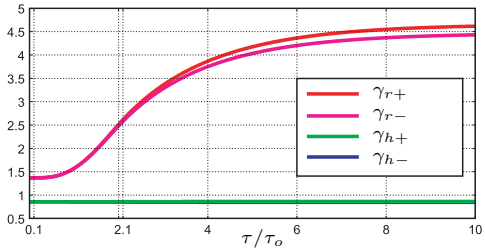

Figure 13: Transformation stretches vs time.

7 Conclusion

We have proposed a mechanical model—a growing spherical shell—suitable for predicting the evolution of a Saccular Cerebral Artery Aneurysms (SCAA), based on three competing remodeling mechanisms—one passive and two active. Despite drastic simplifying assumptions, preliminary numerical experiments attest to the potential of our model to account for nontrivial evolutions ensuing from accidental perturbations of a homeostatic state.

References

[1] A. DiCarlo and S. Quiligotti, *Growth and balance*, Mechanics Research Communications **29** (2002), no. 6, 449–456.

[2] J.D. Humphrey, *Cardiovascular solid mechanics: Cells, tissues, and organs*, Springer, New York, NY, 2001.

[3] S.K. Kyriacou and J.D. Humphrey, *Influence of size, shape and properties on the mechanics of axisymmetric saccular aneurysms*, Journal of Biomechanics **29** (1996), no. 8, 1015–1022, erratum 30: 761, 1997.